Electronic Supplementary Material (ESI) for ChemComm.
This journal is © The Royal Society of Chemistry 2015

Electronic Supplementary Information

Simple synthesis of urchin-like Pt-Ni bimetallic nanostructures as enhanced electrocatalysts for oxygen reduction reaction †

Kwang-Hyun Choi,‡[ab] Youngjin Jang,‡[ab] Dong Young Chung,‡[ab] Pilseon Seo,[ab] Samuel Woojoo Jun,[ab] Ji Eun Lee,[ab⊥] Myoung Hwan Oh,[ab] Mohammadreza Shokouhimehr,[ab] Namgee Jung,[c] Sung Jong Yoo,[d] Yung-Eun Sung*[ab] and Taeghwan Hyeon*[ab]

Experimental Details

Materials. Benzyl ether, hexadecylamine, 1-adamantane carboxylic acid, and nickel acetylacetonate ($Ni(acac)_2$) were purchased from Aldrich Chemical Co. Platinum acetylacetonate ($Pt(acac)_2$) was purchased from Strem. These chemicals were used without further purification.

Synthesis of the urchin-like Pt-Ni nanostructures. The Pt-Ni nanostructures were synthesized by using a heat-up process of a mixture containing $Pt(acac)_2$, $Ni(acac)_2$, hexadecylamine, and 1-adamantane carboxylic acid. In a typical synthesis for Pt_2Ni nanostructures, 50 mg of $Pt(acac)_2$ (0.13 mmol), 17 mg of $Ni(acac)_2$ (0.065 mmol), 1 g of hexadecylamine (4.14 mmol), and 0.144 g of 1-adamantane carboxylic acid (0.8 mmol) were dissolved in 10 ml of benzyl ether and the reaction mixture was degassed under vacuum for 1 h. Then, under Ar atmosphere, the mixture was heated up to 240 ^oC at the heating rate of 4 ^oC/min and then kept at the same temperature for 30 min. After the vessel was cooled, the mixture solution was washed by adding EtOH. After washing twice, the products were dispersed in an organic solvent such as hexane or chloroform. To synthesize Pt_3Ni and PtNi nanostructures, 11 mg and 33 mg of $Ni(acac)_2$ were added, respectively keeping the other conditions the same.

Electrochemical Measurements. The urchin-like Pt-Ni nanostructures with three different molar ratios (Pt:Ni ratios of 1:1, 2:1, and 3:1) were loaded on to a carbon support (Vulcan XC-72) via a hexane solution at a weight ratio of 20% Pt-Ni bimetallic nanostructures to 80% carbon support. The Pt-Ni bimetallic nanostructures were added to 300 ml of hexane, sonicated for 2 h, and stirred overnight. The Pt-Ni loading and atomic composition ratio on the carbon support were measured by TGA analysis (TA5000/SDT Q600). Electrochemical measurements were conducted in an Autolab potentiostat (PGSTA101) using a conventional three-electrode electrochemical cell comprising a platinum wire counter electrode, saturated calomel reference electrode (SCE), and glassy carbon (GC) RDE working electrode at ambient temperature. The electrochemical characteristics and oxygen reduction activity of the urchin-like Pt-Ni nanostructures and commercial Pt (20 wt%; J.M.) were obtained by cyclic voltammetry (CV) and rotating disk electrode (RDE, disk area: 0.196 cm^2) measurements in a 0.1 M $HClO_4$ solution and a 0.5 M H_2SO_4 solution. All of the potentials are versus the reversible hydrogen electrode (RHE) through hydrogen oxidation/evolution potential with Pt disk electrode. Ink was prepared by mixing nanocatalyst, Nafion ionomer and 2-isopropanol. Ink was deposited onto electrode and dried to form a uniform film. The total metal loading level was 16.0 μgcm^{-2}. Before the measurement, 40 potential sweeps between 0.05 to 1.0 V vs. RHE conducted to prepare clean surface and reproducible condition. CV was acquired in the potential range from

0.05 to 1.00 V vs. RHE. Oxygen reduction reaction (ORR) polarization curves were obtained using a RDE 1,600 rpm, with scanning potential ranging from 0.05 to 1.05 V vs. RHE at a scan rate of 10 mV s^{-1} in 0.1 M $HClO_4$ solution under an O_2 flow at 298 K. We compensate the non-faradaic charge/discharge through blank CV (potential sweep between 0.05 to 1.05 V vs. RHE with 10 mVs^{-1} in Ar saturated condition) Further to get the kinetic current, we compensate the ohmic resistance by measuring the impedance at open circuit voltage and assumed constant during measurement. Electrochemical impedance spectroscopy was measured at open circuit potential with an ac 5 mV amplitude, and the frequency range was 100 kHz to 50 mHz. To calculate the kinetic current density, Koutecky-Levich equation is applies as follows:

$$\frac{1}{i} = \frac{1}{i_k} + \frac{1}{i_l}$$

where, i is the total current, i_k is the kinetic current and i_l is the limiting current. The electrochemical surface area was calculated by the calculation of H_{upd} (upd: underpotential deposition) region where potential is below the 0.4 V vs. RHE. To confirm the surface structure of nanoparticle, CV was measured in 0.5 M H_2SO_4 solution under Ar saturated electrolyte at 298 K. The accelerated durability test was conducted with potential sweep method in Ar saturated condition (0.6-1.0 V vs. RHE, 50mVs^{-1} at 298 K)

Characterization. All the transmission electron microscopy (TEM) and the high-resolution TEM (HRTEM) images were obtained using a JEOL EM-2010 and Tecnai F-20 microscope at an accelerating voltage of 200 kV. Energy-filtered TEM (EF-TEM) and HRTEM were conducted using a JEOL-2200FS equipped with an image Cs corrector. The powder X-ray diffraction (XRD) patterns were obtained by a Rigaku D/Max-3C diffractometer (Cu Kα radiation, λ = 0.15418 nm). The elemental analysis was performed by inductively coupled plasma atomic emission spectroscopy (ICP-AES) on an ICPS-7500 spectrometer (Shimadzu). The X-ray absorption fine structure (XAFS) data of the Pt L_{III} edge were obtained on the 7D beamline at the Pohang Light Source (PLS).

Spontaneous removal of the surfactant. The presence of the organic surfactant on the surface of as-prepared urchin-like PtNi nanostructures was investigated by X-ray photoelectron spectroscopy (XPS) and the result is shown in Figure S9. It is known that alkylamine has good binding affinity onto both the Pt and Ni surface (*J. Chem. Sci.* **2004**, *116*, 293; *Nano Lett.* **2001**, *1*, 565) and we used excess amount of 1-hexadecylamine as the surfactant in the synthesis. However, nitrogen signal is not detected from the nanostructures (Figure S9c), which means almost perfect removal of amine from their surface after the synthesis. Also we observed that the colloidal stability of the nanostructures is rapidly decreased as they are dispersed in organic solvent which leads to total precipitation of the nanostructures within a day. We believe that this spontaneous desorption of the amine surfactant is related to the dissolution of Ni from the surface of the Pt-Ni nanostructures dispersed in hexane which we discussed in the main text (Ref. 15 in the main text). As Ni atoms are etched out from the surface of Pt-Ni nanostructures, the amine surfactant can be also detached along with Ni atoms. At the same time, coordination of amine to dissolved Ni atoms in the solution will prevent re-absorption of free amine to the surface of the nanostructures.

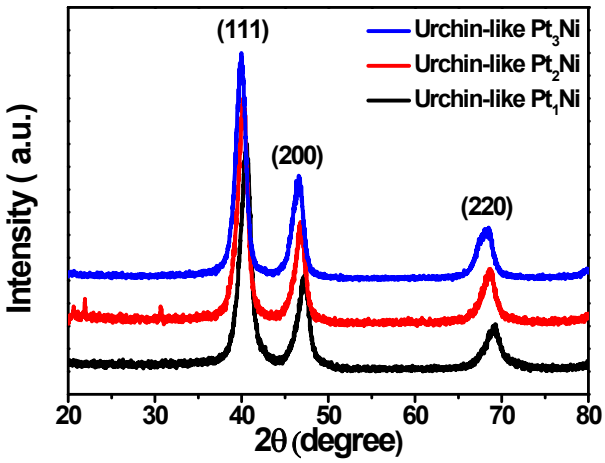

Fig. S1 XRD patterns of the urchin-like Pt-Ni bimetallic nanostructures with three different compositions.

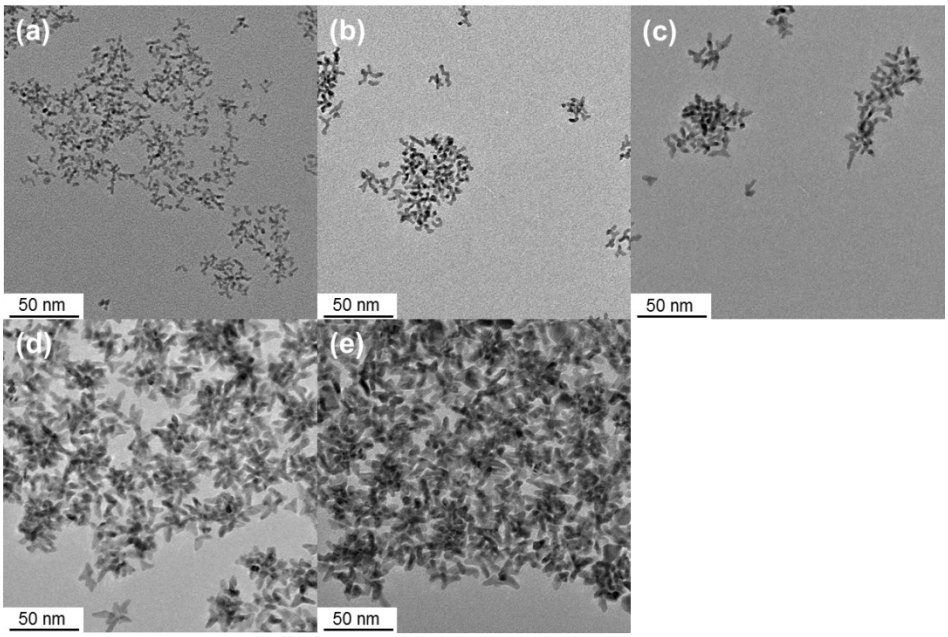

Fig. S2 TEM images of samples taken at different reaction stages: (a) 220 °C, (b) 230 °C, (c) 240 °C, (d) 240 °C and 15 min aging, and (e) 240 °C and 30 min aging.

Table S1. Molar ratios of Pt and Ni at different stages during the synthesis of the Pt_2Ni

nanostructures.

Stage	220 °C	230 °C	240 °C, 0 min	240 °C, 15 min	240 °C, 30 min
Pt:Ni	Only Pt	6.02:1	3.29:1	2.06:1	2.00:1

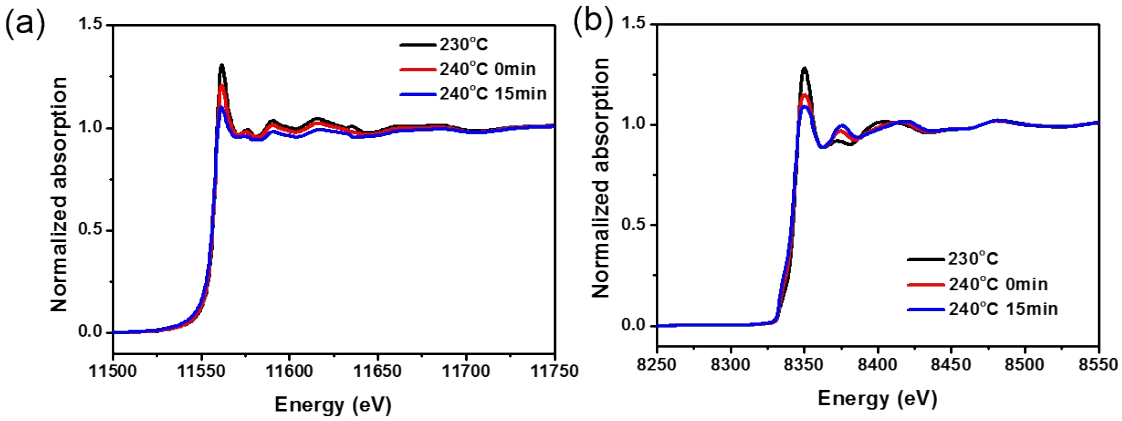

Fig. S3 XANES spectra of the Pt L_{III} edge and Ni k edge during the synthesis of the urchin-like Pt_2Ni nanostructures.

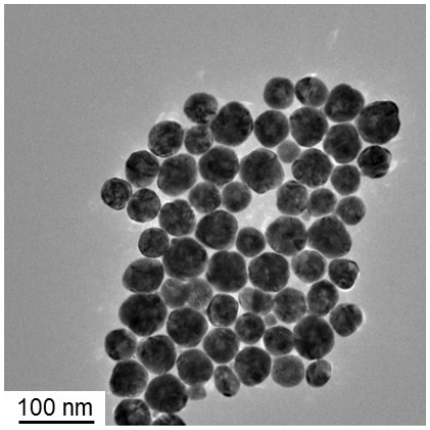

Fig. S4 TEM image of Pt particles synthesized with only $Pt(acac)_2$, which was added under the same synthesis conditions as those for the other Pt-Ni nanostructures.

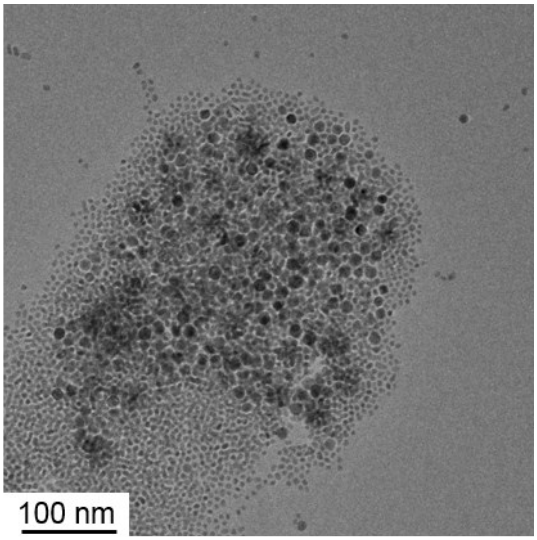

Fig. S5 TEM images of the products synthesized at 260 °C

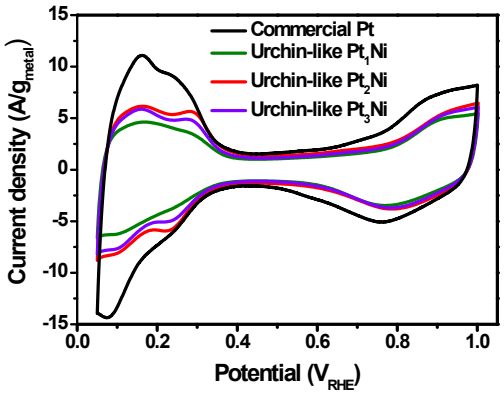

Fig. S6 Cyclic voltammograms of Pt_xNi nanostructures with three different compositions (x=1, 2, and 3) and the reference commercial Pt catalyst in $HClO_4$ electrolyte.

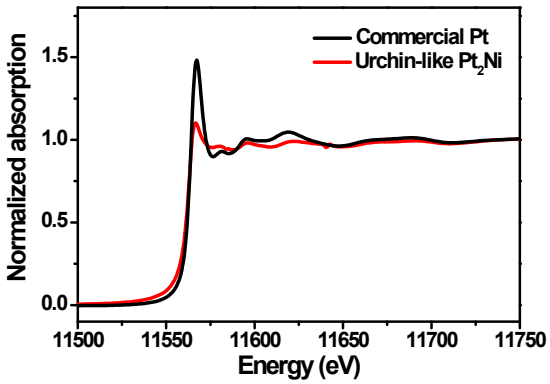

Fig. S7 Pt L3 edge XANES results of commercial Pt and urchin-like Pt_2Ni.

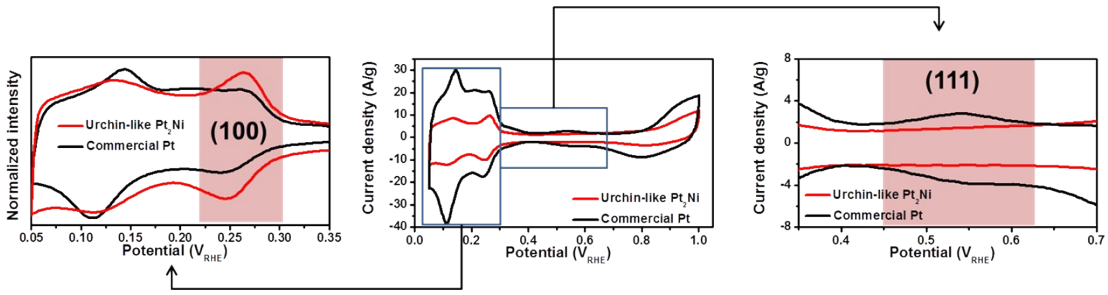

Fig. S8 Cyclic voltammograms of the urchin-like Pt_2Ni catalyst and the commercial Pt catalyst in H_2SO_4 electrolyte.

Table S2. Accelerated durability test (ADT) results

	Initial mass activity (A/mg^{-1})	After mass activity (A/mg^{-1})	Activity loss (%)	Half wave potential change(mV)
Commercial Pt/C	0.13	0.042	68 %	28
Commercial Pt_3Ni/C	0.20	0.037	81 %	60
Urchin-like Pt_2Ni/C	1.59	0.688	57 %	23

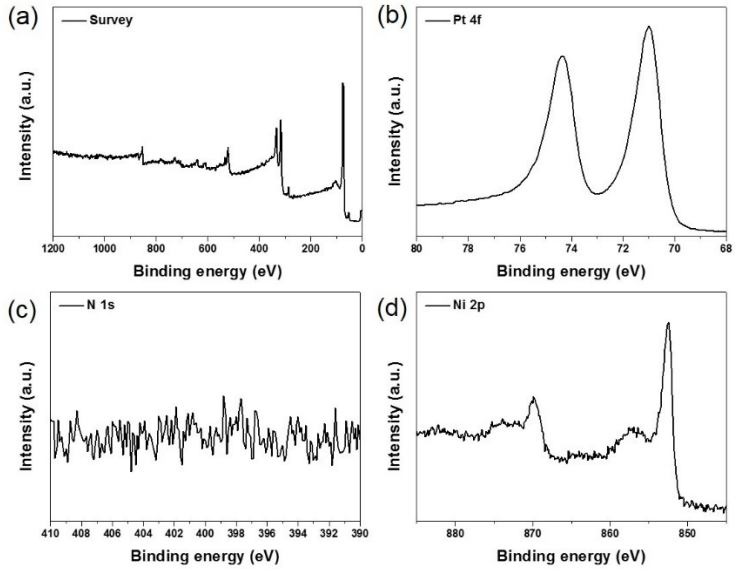

Fig. S9 XPS results of the urchin-like Pt_2Ni catalyst. (a) Survey, (b) Pt 4f, (c) N 1s and (d) Ni 2p signal. (XPS measured after synthesis of nanoparticle)

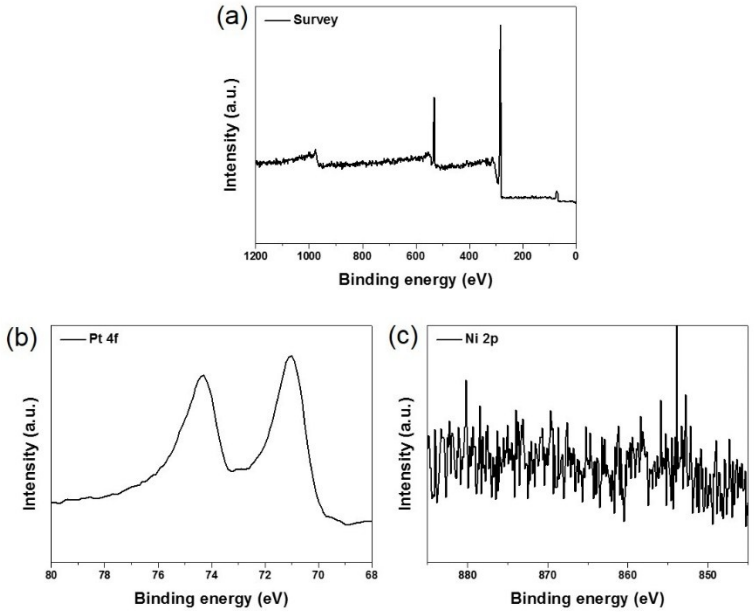

Fig. S10 XPS results of the urchin-like Pt_2Ni catalyst. (a) Survey, (b) Pt 4f, (c) Ni 2p signal. (XPS measured after nanoparticles are loaded on to the Vulcan XC-72R)

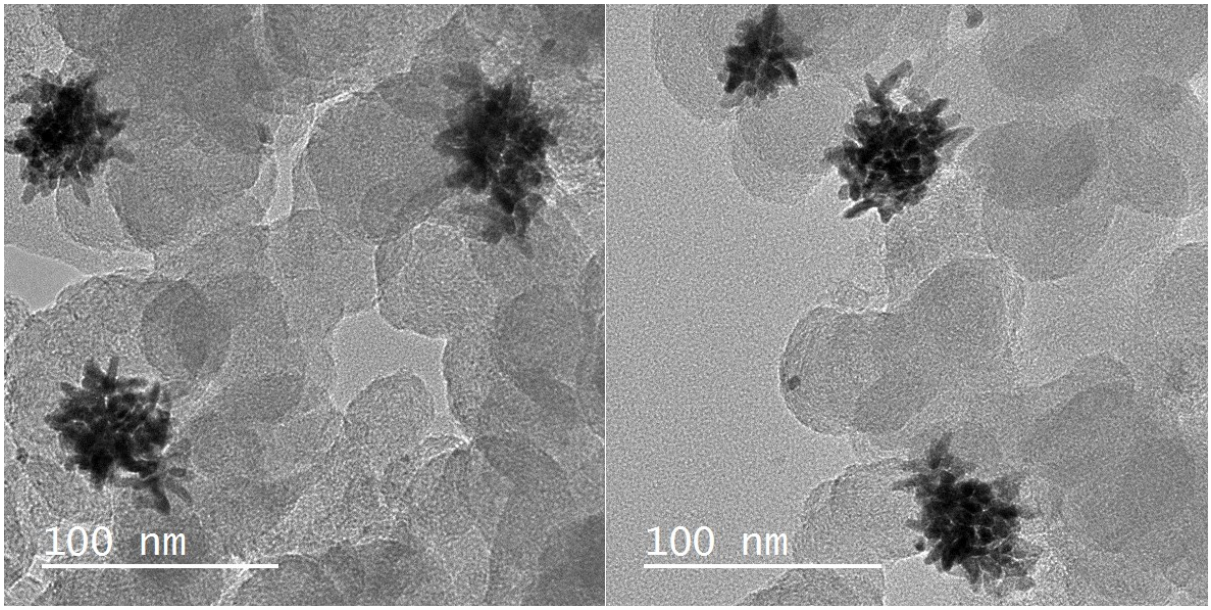

Fig. S11 TEM images after deposition to carbon support

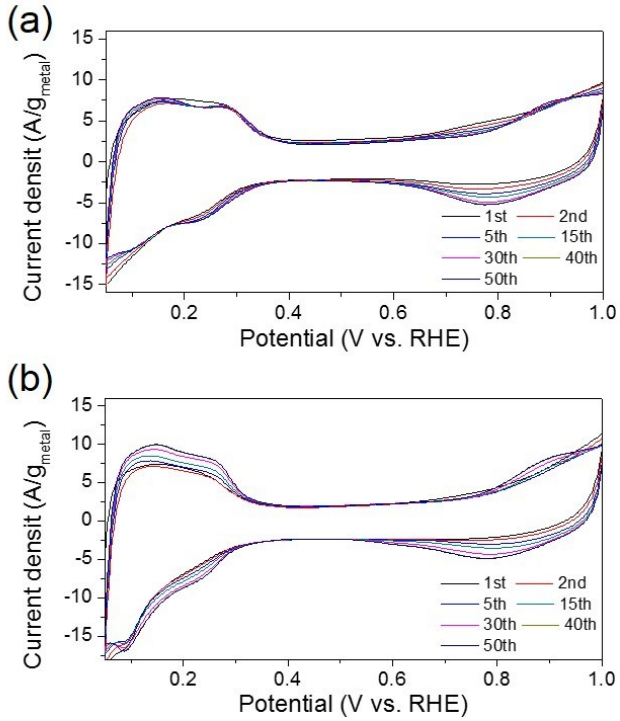

Fig. S12 CV pre-cycling of (a) urchin-like Pt_2Ni/C and (b) commercial Pt_3Ni/C

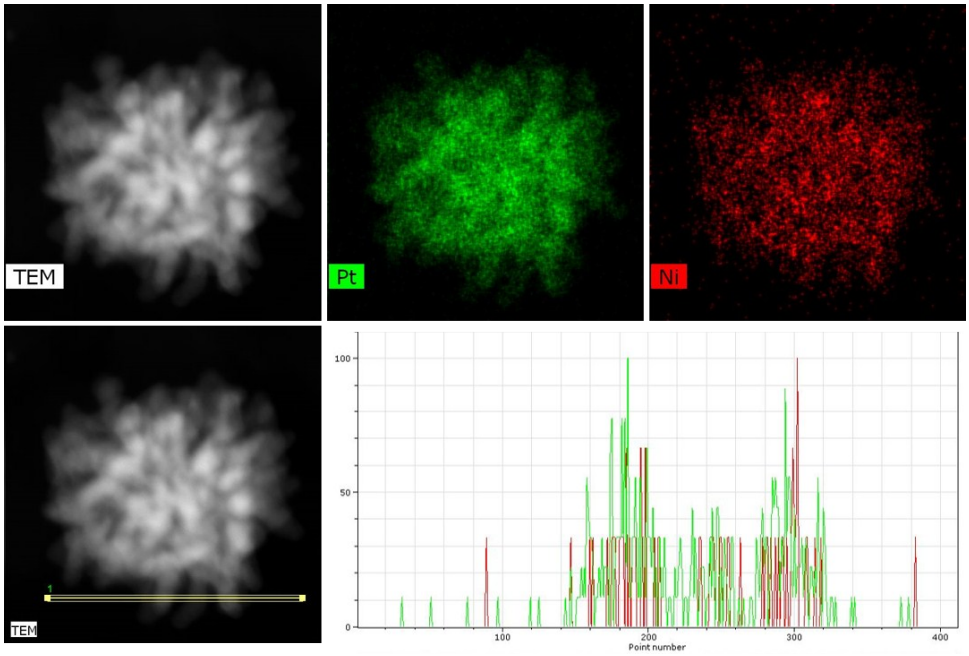

Fig. S13 STEM EDS results of urchin-like Pt_2Ni nanoparticles after ADT test and line scan analysis

Table S3. Molar ratios of Pt_2Ni nanostructures before and after ADT

	Pt	Ni
Urchin-like Pt_2Ni/C_initial	69	31
Urchin-like Pt_2Ni/C_after ADT	76	24